RSC Advances

PAPER

Cite this: *RSC Adv.*, 2022, **12**, 25068

Synthesis and antibacterial activity studies *in vitro* of indirubin-3′-monoximes†

Fen-Fen Yang,‡[a] Ming-Shan Shuai,‡[a] Xiang Guan,[a] Mao Zhang,[a] Qing-Qing Zhang,[a] Xiao-Zhong Fu,[a] Zong-Qin Li,[c] Da-Peng Wang,[b] Meng Zhou,[a] Yuan-Yong Yang,[a] Ting Liu,[a] Bin He[a] and Yong-Long Zhao*[a]

Multi-drug-resistant microbial pathogens are a serious global health problem. New compounds with antibacterial activity serve as good candidates for developing novel antibacterial drugs which is very urgent and important. In this work, based on the unique scaffold of indirubin, an active ingredient of traditional Chinese medicine formulation Danggui Luhui Wan, we synthesized 29 indirubin-3′-monoximes and preliminarily evaluated their antibacterial activities. The antibacterial activity results demonstrated that the synthesized indirubin-3′-monoximes **5a–5z** and **5aa–5ad** displayed good potency against *S. aureus* ATCC25923 (MIC = 0.4–25.6 μg mL^{-1}). Among them, we found that the 5-F, 5-Cl and 7-CF_3 substituted indirubin-3′-monoximes **5r**, **5s** and **5aa** also showed better antibacterial efficiency for *S. aureus* (MICs up to 0.4 μg mL^{-1}) than the prototype natural product indirubin (MIC = 32 μg mL^{-1}). More importantly, indirubin-3′-monoxime **5aa** has certain synergistic effect with levofloxacin against clinic multidrug-resistant *S. aureus* (fractional inhibitory concentration index: 0.375). In addition, relevant experiments including electron microscopy observations, PI staining and the leakage of extracellular potassium ions and nucleic acid (260 nm) have been performed after treating *S. aureus* with indirubin-3′-monoxime **5aa**, and the results revealed that indirubin-3′-monoximes could increase the cell membrane permeability of *S. aureus*. Although indirubin-3′-monoxime **5aa** showed some cytotoxicity toward SH-SY5Y cells relative to compounds **5r** and **5s**, the skin irritation test of male mice after shaving showed that compound **5aa** at a concentration of 12.8 μg mL^{-1} had no toxicity to mouse skin, and it could be used as a leading compound for skin antibacterial drugs.

Received 16th February 2022
Accepted 21st August 2022

DOI: 10.1039/d2ra01035f

rsc.li/rsc-advances

Introduction

With the indiscriminate use of antibiotics, antibiotic-resistant pathogens (such as ESKAPE pathogens: *Enterococcus faecium*, *Staphylococcus aureus*, *Klebsiella pneumoniae*, *Acinetobacter baumannii*, *Pseudomonas aeruginosa*, and *Enterobacter* spp.)[1–3] have become an issue of great concern worldwide which seriously threatens global public health safety.[1–12] According to statistics, there is an annual death toll worldwide of 700 000 caused by antimicrobial resistance, and this value is expected to increase to up to 10 million in 2050.[4–7] As a consequence, there is an urgent and growing need for the development of novel antibacterial drugs to overcome bacterial resistance.[1] For pharmaceutical companies, most of them are not interested in the research and development program of new antibiotics due to their high costs and low profits.[1,8] So the development and identification of new compounds with the antibacterial activity that serve as good candidates for developing novel antibacterial drugs are very urgent and important.[1,8]

Chinese medicine and pharmacology have a 5000 year-old tradition in China.[13,19] Bioactive plant constituents, especially from medicinal plants used in traditional Chinese medicine (TCM), are also playing an increasingly important role in the process of current drug discovery and innovation.[6,13–18] A classic success example is the world-famous antimalarial drug named artemisinin, which was also named "Qinghaosu" in China and was isolated and identified by Youyou Tu and coworkers from the TCM plant "Qinghao" *via* some popular empirical formulas in some regions and the old documentation in the TCM literature. Due to the significant contribution to the discovery of artemisinin and fighting malaria, Youyou Tu became the first Chinese Nobel Laureate in Physiology or Medicine in 2015.[14]

[a]*State Key Laboratory of Functions and Applications of Medicinal Plants, School of Pharmacy, and Engineering Research Center for the Development and Application of Ethnic Medicine and TCM (Ministry of Education), Guizhou Medical University, Guiyang 550004, People's Republic of China. E-mail: zhaoyl05@126.com; zhaoyonglong@gmc.edu.cn; 378122847@qq.com*

[b]*Key Laboratory of Environmental Pollution Monitoring and Disease Control, Ministry of Education, Guizhou Medical University, Guiyang, 550025, People's Republic of China*

[c]*Department of Neurology, Sichuan Mianyang 404 Hospital, Mianyang, 621000, People's Republic of China*

† Electronic supplementary information (ESI) available. See https://doi.org/10.1039/d2ra01035f

‡ These authors made equal contributions to this work.

Similar to bioactive plant constituent artemisinin, indirubin (Fig. 1A) is also the active plant ingredient of indigo naturalis (named Sei Tai in Japanese or Qing Dai in Chinese, a dark blue powder prepared from the leaves and branches of various indigo-producing plants)[17,19–27] and Danggui Luhui Wan (a TCM formulation in the treatment of various chronic diseases such as cancer and inflammation, and composed of 11 medicinal herbs including indigo naturalis, *etc.*).[20–23] Indirubin has the interesting 3,2′-bisindole scaffold and shows multiple biological properties,[19–23] including hemostatic, anticancer, antipyretic, anti-inflammatory, sedative, antibacterial, and antiviral properties.[22,23] However, due to the existence of a hydrogen-bonding framework in the structure of indirubin, the property of extremely poor solubility in most solvents has been observed, which is the main obstacle for the clinical application of indirubin.[21,28–36]

Up to now, much effort has been focused on indirubin and its derivatives; in particular, various cellular targets have been found including CDKs,[19,37,38] GSK-3β,[39] VEGFR-2,[40] c-Src,[41–43] Dyrk1A,[44] and other kinases.[15,45,46] Despite this, current research on indirubins is still mainly focused on the improvement of their water solubility and cytotoxicity.[21,28–36,47] At present, although a few examples of the antimicrobial activity of indirubin and indigo extract from indigo naturalis or *Wrightia tinctoria* have been reported, post-modified indirubin antibacterial agents have not been reported.[48–54] Indirubin-3′-monoxime is a synthetic derivative of indirubin and is usually used as a key intermediate for the synthesis of water-soluble indirubins.[22,28,55] In addition, indirubin-3′-monoximes also have various biological properties and can inhibit the activities of CDKs, GSK-3β, 5-lipoxygenase, *etc.*[19,22,29,38,55–59] However, to the best of our knowledge, there are no reports related to antimicrobial research on indirubin-3′-monoximes. With our ongoing interest in the new uses and in-depth development of indirubins,[29] we hereby synthesized a series of indirubin-3′-monoximes and investigated their related antibacterial activity (Fig. 1B).

Results and discussion

Chemistry

Based on our previous research work on indirubin derivatives[29] and related literature reports,[19,22,38,55–59] the syntheses of indirubin-3′-monoximes **5a–z** and **5aa–5ad** have been realized *via* the related synthesis routes as shown in Scheme 1. Firstly, starting from various substituted 2-bromobenzoic acids **1a–m**, corresponding dicarboxylic acids **2a–m** were synthesized *via* copper-catalyzed aromatic amination reaction with glycine (Scheme 1a). Then, various substituted 3-indoxyl acetates **3a–m** were synthesized *via* the intramolecular cyclization of dicarboxylic acids **2a–m** in the presence of acetic anhydride (Scheme 1b). Next, the acidic condensation of different substituted 3-indoxyl acetates **3a–m** as key intermediates with various isatins **6a–m** yielded the corresponding indirubins **4a–m** and **7a–m** (Scheme 1c). Finally, the target indirubin-3′-monoximes **5a–z** and **5aa–5ad** could be easily prepared *via* heating the synthetic indirubins **4a–m** and **7a–m** with hydroxylamine hydrochloride in pyridine (Scheme 1d).

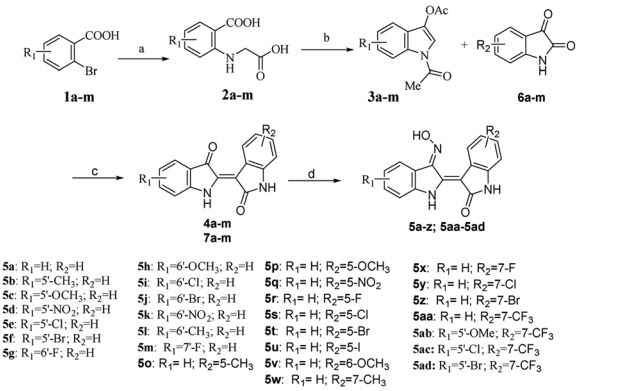

Scheme 1 The synthesis of indirubin-3′-monoximes **5**.

In vitro antibacterial activity of indirubin-3′-monoximes 5a–z and 5aa–5ad

The minimum inhibitory concentrations (MICs) of synthetic indirubin-3′-monoximes were tested against Gram-positive (G^+) bacteria (*S. aureus* ATCC25923 and clinically isolated multidrug-resistant *S. aureus* 20 151 027 077) and Gram-negative (G^-) bacteria (*E. coli* ATCC25922 and *Pseudomonas aeruginosa* ATCC9027) through broth microdilution procedures described in the Clinical and Laboratory Standards Institute (CLSI) 2018 standard methodology.[62,67–69] MIC values for synthetic indirubin-3′-oximes were compared with those for reference drugs levofloxacin and indirubin under the same assay conditions for antimicrobial susceptibility assessment. In general, most of indirubin-3′-monoximes showed stronger antibacterial

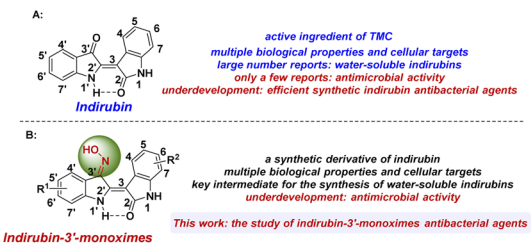

Fig. 1 Research status of indirubin and indirubin-3′-monoximes.

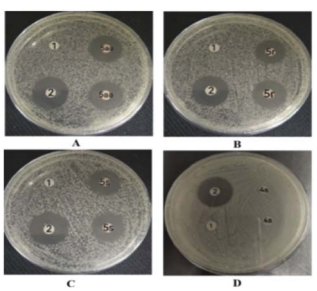

Fig. 2 Images of antibacterial zones of DMSO (**1**), levofloxacin (**2**), and (D) **4a**, (A) **5aa**, (B) **5r** and (C) **5s** against *S. aureus* ATCC25923.

Table 1 MIC (μg mL^{-1}) of synthetic indirubin-3′-oximes

Compound	Minimum inhibitory concentration/MIC (μg mL^{-1})			
	S. aureus ATCC25923	*E. coli* ATCC25922	*P. aeruginosa* ATCC9027	*S. aureus*[b] 20 151 027 077
Lev.[a]	<0.2	<0.2	12.5	16
Indirubin (**4a**)	32/12.5[c]	>200	>200	>200
5a	16	>200	>200	>200
5b	1.6	>200	>200	>200
5c	0.8	>200	25.6	>200
5d	3.2	>200	>200	>200
5e	0.8	>200	>200	>200
5f	0.8	>200	>200	>200
5g	3.2	>200	>200	>200
5h	6.4	>200	>200	>200
5i	3.2	>200	>200	>200
5j	3.2	>200	>200	>200
5k	6.4	>200	>200	>200
5l	12.5	>200	>200	>200
5m	25.6	>200	>200	>200
5o	3.2	>200	>200	>200
5p	3.2	>200	>200	>200
5q	12.8	>200	>200	>200
5r	0.4	>200	>200	>200
5s	0.4	>200	>200	>200
5t	0.8	>200	>200	>200
5u	3.2	>200	>200	>200
5v	1.6	>200	>200	>200
5w	6.4	>200	128	>200
5x	1.6	>200	>200	>200
5y	3.2	>200	>200	>200
5z	1.6	>200	128	>200
5aa	0.4	>200	>200	>200
5ab	12.8	>200	>200	>200
5ac	1.6	>200	>200	>200
5ad	3.2	>200	>200	>200

[a] Lev. is levofloxacin. [b] Clinical isolated multidrug-resistant bacterial strain. [c] MIC value reported in ref. 49.

Table 2 Comparison of MIC and MBC values for **5r**, **5s** and **5aa** against *S. aureus* ATCC25923[a]

Compound	MBC (μg mL^{-1})	MIC (μg mL^{-1})	MBC/MIC
Levofloxacin	<0.4	<0.2	<2
5aa	6.4	0.4	16
5r	12.8	0.4	32
5s	12.8	0.4	32

[a] Bactericidal behavior: MBC/MIC ratio = 1 to 2; bacteriostatic behavior: MBC/MIC ratio ≥ 8.

activities against *S. aureus* ATCC25923 than indirubin (MIC = 32 μg mL^{-1} or 12.5 μg mL^{-1} (ref. 49)). Except that compounds **5c**, **5w** and **5z** showed certain antibacterial activities against *P. aeruginosa* ATCC9027 (with MIC values of 25.6, 128, and 128 μg mL^{-1}, respectively), most of the indirubin-3′-monoximes have no obvious antibacterial effects on clinically isolated multidrug-resistant *S. aureus* 20 151 027 077 and G^{-} bacterial strains (*E. coli* ATCC25922 and *P. aeruginosa* ATCC9027). For the antibacterial activities against *S. aureus* ATCC25923, we first investigated the effects of different R^1 groups at 5′, 6′ and 7′ positions of indirubin-3′-monoximes (**5a–m**). The results revealed that indirubin-3′-monoximes with electron-donating (such as OMe and Me) and halide (such as Cl and Br) substitutions at C5′ position showed good antibacterial activities and the MIC values of corresponding 5′-OMe, 5′-Cl and 5′-Br substituted compounds **5c**, **5e** and **5f** up to 0.8 μg mL^{-1}. For R1 substituents at C6′ position, the antibacterial activities of indirubin-3′-monoximes (**5g**, **5i** and **5j**) substituted by halogen atoms (such as 5′-F, Cl and Br) were better than those of other indirubin-3′-monoximes (**5h**, **5k** and **5l**) substituted with electron-donating (6′-OMe and Me) or electron-withdrawing (6′-NO_2) groups. In addition, indirubin-3′-monoximes **5a–z** and **5aa** with different R^2 groups at 5, 6 and 7 positions were also tested. In addition to 5-I substituted compound **5u**, whether C5 is an electron-withdrawing (NO_2) or electron-donating (Me, OMe) substituent, the antibacterial activities against *S. aureus* ATCC25923 of indirubin-3′-monoximes substituted by halogen atoms at C5 are better (**5r–t** *vs.* **5o–q**), and the MIC values of 5-F substituted compound **5r** and 5-Cl substituted compound **5s** were also up to 0.4 μg mL^{-1}. For R^2 substituents at C7 position,

Table 3 *In vitro* antibacterial activity of indirubin-3′-monoximes used alone or in combination with levofloxacin against a multidrug-resistant bacterial strain of *S. aureus* (20 151 027 077) by the checkerboard microdilution assay

	Levofloxacin					
Compound	Alone	Synergetic	Alone	Synergetic	FICI[a]	Interpretation
Indirubin (**4a**)	256	128	16	8	1	Additive
5r	256	128	16	4	0.75	Additive
5s	256	128	16	8	1	Additive
5aa	256	64	16	2	0.375	Synergistic

[a] The interaction as reflected by FICI values: synergistic (FICI $\leq$ 0.5), additive (0.5 < FICI $\leq$ 1), indifferent (1 < FICI $\leq$ 4) and antagonistic (FICI > 4).

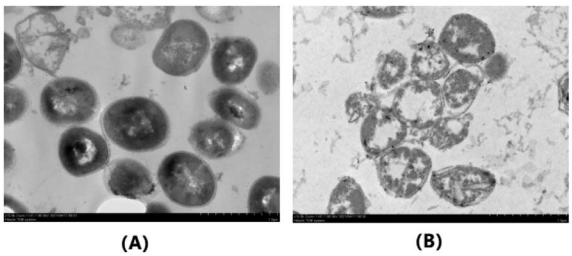

Fig. 3 TEM images of *S. aureus* ATCC25923 cells. (B) Treated with **5aa** at 12.8 μg/mL for 16 h; (A) blank control (magnification, ×15 000).

indirubin-3′-monoximes substituted with electron-withdrawing substituents showed good antibacterial activities against *S. aureus* ATCC25923 and the MIC value of 7-CF3 substituted compound **5aa** was also up to 0.4 μg mL^{-1}. Based on the size of bacteriostatic ring of synthetic compounds **5r**, **5s** and **5aa**, compound **5aa** with an electron-withdrawing CF_3 substituent at C7 position was chosen as the model compound for further study (Fig. 2). Considering the effect of R^1 and R^2 groups in the structure of indirubin-3′-monoximes on antibacterial activities, we further synthesized compounds **5ab–5ad** to find indirubin-3′-monoximes with more efficient antibacterial activities. However, it was regrettable that the antibacterial activities against *S. aureus* ATCC25923 of compounds **5ab–5ad** still did not exceed that of compound **5aa**.

Determination of antibacterial zone diameter

To further validate the antimicrobial effect of the above-mentioned drug sensitivity test more intuitively, we quantitatively and qualitatively evaluated the antibacterial activities of synthetic indirubin-3′-monoximes **5r**, **5s** and **5aa** on *S. aureus* ATCC25923 by measuring the diameter of the inhibition zone *in vitro*. The size of the inhibition ring was positively correlated with the drug concentration, that is, with an increase of the compound concentration, the inhibition zone diameter increased. As shown in Fig. 2, it could be observed that at the same concentration (12.8 μg mL^{-1}) of levofloxacin (**2**) and compounds **5r**, **5s** and **5aa**, the bacteriostatic ring sizes of levofloxacin (21.7 mm), **5aa** (19.0 mm), **5r** (18.5 mm) and **5s** (18.3 mm) were obtained. However, colonies occurred on the medium containing both negative control DMSO and leading compound indirubin (**4a**) at the same concentration. Thus, compounds **5r**, **5s** and **5aa** effectively inhibited the emergence of *S. aureus* ATCC25923.

The bactericidal or bacteriostatic assay of indirubin-3′-monoximes

With the better MICs of synthetic indirubin-3′-monoximes **5r**, **5s** and **5aa** against *S. aureus* ATCC25923 in Table 1, we also tested the MBC (minimal bactericidal concentration) values and obtained the corresponding MBC/MIC ratios of these indirubin-3′-monoximes to further investigate whether their activity was bactericidal or bacteriostatic. According to the CLSI standards (bactericidal behavior: MBC/MIC ratio = 1 to 2; bacteriostatic behavior: MBC/MIC ratio $\geq$ 8),[69,70] the results as shown in Table 2 indicated that indirubin-3′-monoximes **5r**, **5s** and **5aa** were also observed as bacteriostatic agents with MBC/MIC ratios of >8.

Indirubin-3′-monoximes in combination with levofloxacin inhibited multidrug-resistant bacterial strain of *S. aureus* (20 151 027 077)

The *in vitro* antibacterial activities of compounds indirubin **4a** and indirubin-3′-monoximes **5r**, **5s** and **5aa** used alone or in combination with levofloxacin were analyzed by a checkerboard microdilution assay (Table 3). As shown in Table 3, indirubin **4a** and indirubin-3′-monoximes **5r**, **5s** and **5aa** generally were inactive in inhibiting the growth of multi-drug-resistant strain *S. aureus* 20 151 027 077 (MIC $\geq$ 200 μg mL^{-1}) when used alone. But, to our delight, indirubin-3′-monoxime **5aa** showed a certain synergistic effect with levofloxacin and the MIC value of levofloxacin was reduced from 16 μg mL^{-1} to 2 μg mL^{-1}, and the corresponding fractional inhibitory concentration index (FICI) value was 0.375.[63,71] The results as shown in Table 3 also indicated that **4a**, **5r** and **5s** also displayed additive effects with levofloxacin in inhibiting the growth of multi-drug-resistant strain *S. aureus* 20 151 027 077, and corresponding FICI values of 0.75 and 1 were obtained, respectively. Thus, indirubin-3′-monoxime **5aa** showed a certain synergistic effect and represents a lead compound as a potential antibacterial synergist for the combination therapy of multi-drug-resistant *S. aureus* infections. At the same time, using a similar method, we also investigated the *in vitro* antibacterial activity of indirubin **4a**, and indirubin-3′-monoximes **5r**, **5s** and **5aa** used alone or in combination with levofloxacin against G^- bacterium *P.*

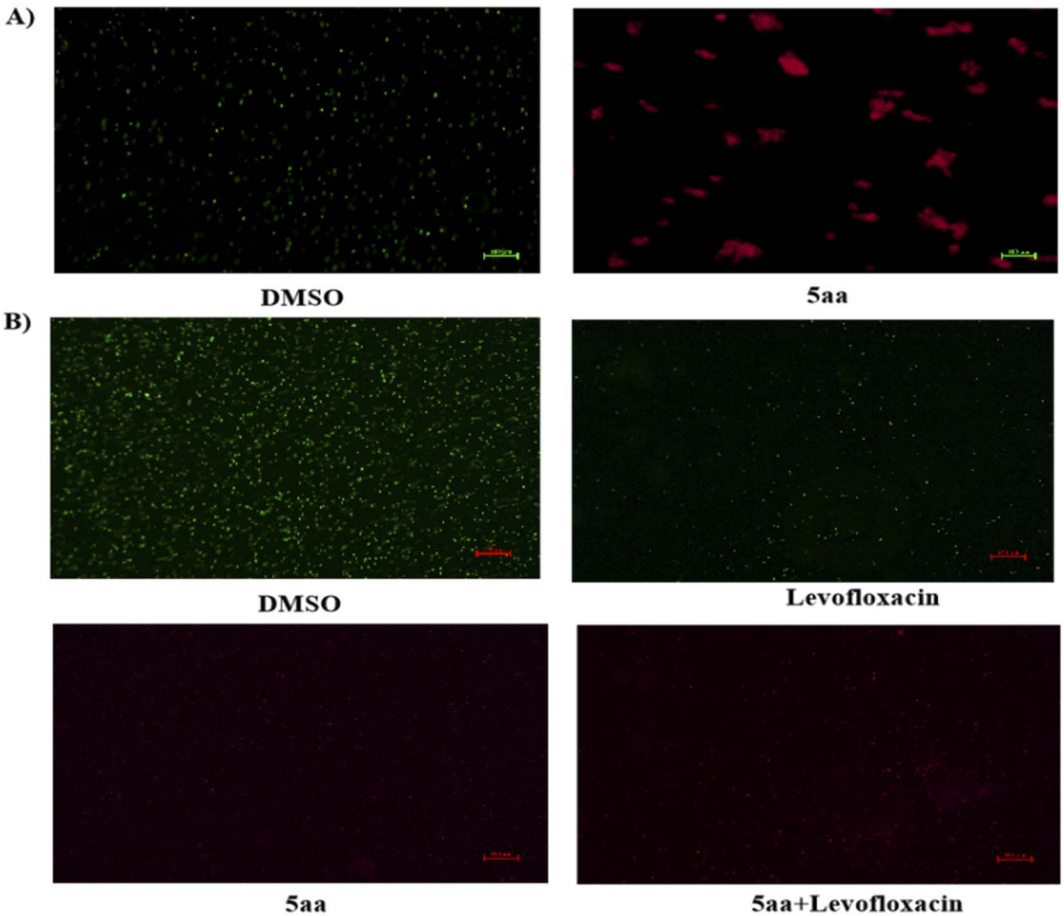

Fig. 4 (A) Fluorescence micrographs of *S. aureus* ATCC 29213 cells treated with 12.8 μg mL^{-1} of **5aa** for 2 h. DMSO treatment served as a negative control. Syto9 stains all cells irrespective of membrane integrity, whereas PI only stains cells with a permeabilized membrane. Bars represent 100 μm (magnification, ×10). (B) Fluorescence micrographs of multi-drug-resistant *S. aureus* 20 151 027 077 cells. Bars represent 100 μm (magnification, ×10).

aeruginosa ATCC9027 and the results also showed indifference effects (FIC index range: 1.5 to 2, see Table S1† in ESI).

Effects of indirubin-3′-monoxime 5aa on external morphology and cell membrane permeability of *S. aureus*

Due to its excellent activity against *S. aureus* (ATCC25923), we further investigated the effect of indirubin-3′-monoxime **5aa** on the external morphological features of *S. aureus* (ATCC25923) cells *via* transmission electron microscopy (TEM) analysis (Fig. 3). As shown in Fig. 3A, the untreated *S. aureus* cells show their spherical and plump connatural morphology and appear normal, both the cytoplasmic membrane and the peptidoglycan layer of the cell wall being retained. In contrast, *S. aureus* cells treated with indirubin-3′-monoxime **5aa** appeared to become empty and show rupture and lysis of the membranes (Fig. 3B). For the *S. aureus* cells treated with **5aa**, it could also be clearly observed in Fig. 3B that there was release of cellular contents into the surrounding environment. Therefore, there are various indications that the antibacterial activity of indirubin-3′-monoxime **5aa** might be related to changes in the structure and permeability of the *S. aureus* cell membrane.

The antibacterial activity of indirubin-3′-monoxime **5aa** indicates that the target of **5aa** may be the cell membrane of bacteria. Thus, the possibility of **5aa** interacting with the bacterial membrane was further investigated by fluorescence microscopy using a double staining approach. *S. aureus* ATCC25923 cells were treated with **5aa** and then costained with Syto9 and PI. PI enters the cell and subsequently intercalates DNA upon loss of membrane integrity.[74] As shown in Fig. 4A, *S. aureus* cells were incubated with a solvent negative control: bacteria were stained using Syto9 showing green fluorescence, while few of them had PI staining (red fluorescence). However, *S. aureus* cells showed a strong red fluorescence as a result of PI staining after incubation with **5aa** for 2 h (Fig. 4A), pointing to the fact that compound **5aa** causes pronounced membrane permeabilization and the bacteriostatic activity of the compound was not related to DNA damage. Membrane permeability by **5aa** combined with levofloxacin against multi-drug-resistant *S. aureus* 20 151 027 077 was further evaluated *via* PI internalization assay. The effects of solvent, levofloxacin, and **5aa** and **5aa** combined with levofloxacin on cells of multi-drug-resistant *S. aureus* 20 151 027 077 incubated with Syto9/PI are depicted in Fig. 4B. **5aa** and **5aa** combined with

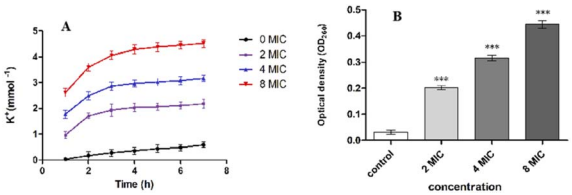

Fig. 5 (A) Effect of treatment with different concentrations of **5aa** on the extracellular amount of potassium leakage for *S. aureus* ATCC25923; bars represent the standard deviation ($n = 3$). (B) Effect of different concentrations of **5aa** on the release rate of 260 nm absorbing material (nucleic acid) from *S. aureus* ATCC25923; data are expressed as mean ± SD ($n = 3$), $p < 0.05$.

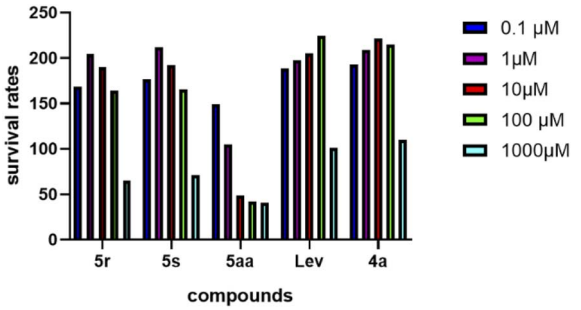

Fig. 6 Cytotoxicity of compounds **5r**, **5s** and **5aa** to SH-SY5Y cells.

levofloxacin instigated a gradual, yet conspicuous increase in fluorescence intensity, showing an ability to permeabilize the bacterial membrane. In contrast, cells incubated with control group solvent and levofloxacin (antibiotic impeding bacterial growth by inhibiting DNA gyrase synthesis) showed very minor to no fluorescence as expected. This result is consistent with the fluorescence microscopy observations.

To further confirm the effect of indirubin-3′-monoxime **5aa** on *S. aureus* cell membrane, we also investigated the leakage of cytoplasmic constituents (such as potassium and nucleic acids) of *S. aureus* (ATCC25923) treated with **5aa**. As shown in Fig. 5, the extracellular K^+ (Fig. 5A) and nucleic acid concentrations (Fig. 5B) were also increased significantly after *S. aureus* (ATCC25923) was treated with different concentrations (2MIC, 4MIC and 8MIC) of **5aa**. These results were consistent with several previous reports, which all revealed that the membrane structure of microorganisms could be damaged by natural components, and these natural components can also promote the loss of cellular components, such as ions, proteins, and nucleic acids.[60,61,64–66,72,73] Therefore, indirubin-3′-monoxime **5aa** might show its antibacterial activity by damaging the cell membrane structure of *S. aureus* (ATCC25923), changing the cell membrane permeability, and eventually leading to the leakage of cytoplasmic constituents such as K^+, nucleic acid, *etc.*

Cytotoxicity results of indirubin-3′-monoximes

To evaluate the safety of these indirubin-3′-monoximes, we investigated the cytotoxicity of compounds **5aa**, **5r** and **5s** on hepatocytes and SH-SY5Y cells. Unfortunately, these indirubin-3′-monoximes showed greater hepatotoxicity. The effect of indirubin-3′-monoximes **5r**, **5s** and **5aa** on SH-SY5Y cells' survival rate at 0.1, 1, 10, 100, 1000 μM is shown in Fig. 6. It can be seen that indirubin-3′-monoximes **5r** and **5s** at 0.1–100 μM have also no obvious cytotoxicity to SH-SY5Y cells. However, indirubin-3′-monoxime **5aa** has a concentration-dependent effect on the survival rate of SH-SY5Y cells. With the increase of **5aa** concentration, the survival rate of SH-SY5Y cells decreased, and the cell survival rate was below 50% at a concentration of 10 μM **5aa**.

Skin irritation test

To further investigate the safety of these indirubin-3′-monoximes, we conducted a skin irritation test of indirubin-3′-monoxime **5aa** on male mice after shaving. Table 4 shows skin tolerance test findings. Mice showed no irritation signs or skin edema after treatment with 12.8 μg mL^{-1} **5aa**. The treated skin was intact, with no inflammation and erythema compared to the untreated site (Fig. 7). No erythema or edema was observed with PII equal to "0" in each mouse at any time of the observation after removing the test material, which indicates that indirubin-3′-monoxime **5aa** is safe for topical use.[76,77] In addition, for the cytotoxicity in hepatocyte cell line, we also analyzed the histopathological section of mice liver tissue after skin irritation test *via* the treatment of **5aa** (12.8 μg mL^{-1}) for 1–72 h and the results also revealed that indirubin-3′-monoxime **5aa** is safe for topical use and has no obvious cytotoxic effects on liver tissue (see ESI†). Nevertheless, due to the multiple biological activities of indirubin-3′-monoximes that we mentioned in the introduction, and the above-mentioned cytotoxicity in hepatocyte cell line and SH-SY5Y cells of **5aa**, the above results only suggest that indirubin-3′-monoxime **5aa** could be used as a leading compound of skin antibacterial drugs, and further in-depth and systematic research (such as in-depth structure–

Table 4 Skin reaction score of indirubin-3′-monoxime **5aa** on male mice after shaving at various time intervals (3 treatment sites)[a]

	1 h		24 h		48 h		72 h	
Reaction	Con	Trt	Con	Trt	Con	Trt	Con	Trt
Erythema	0	0	0	0	0	0	0	0
Edema	0	0	0	0	0	0	0	0

[a] Primary Irritation Index (PII) = 0/3; PII = 0, based on PII irritation category for indirubin-3′-monoxime 5aa being negligible.

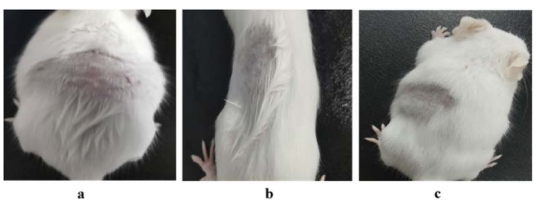

Fig. 7 Skin irritation in mice. (a) Untreated mouse. (b) Mouse treated with 12.8 μg mL^{-1} **5aa** for 1 h. (c) Mouse treated with 12.8 μg mL^{-1} **5aa** for 24 h.

activity relationship research) on antibacterial activity, and thorough and further toxicological studies (such as the mutagenic (genotoxic) potential, carcinogenic, reproductive and developmental toxicity, and neurotoxicity) are still needed for other types of antibacterial uses of indirubin-3′-monoximes.

Conclusions

In this work, we synthesized a series of indirubin-3′-monoximes and preliminarily evaluated their antibacterial activities. Among them, we found that the synthesized indirubin-3′-monoximes **5r**, **5s** and **5aa** displayed better anti-*S. aureus* ATCC25923 (MIC up to 0.4 μg mL^{-1}) activity than indirubin (MIC = 32 μg mL^{-1}). More importantly, indirubin-3′-monoxime **5aa** showed a certain synergistic effect with levofloxacin against clinic multidrug-resistant *S. aureus* 20 151 027 077 (FICI: 0.375), which could be used as a lead compound as a synergistic antibacterial agent of levofloxacin for the combination therapy of multi-drug-resistant *S. aureus* infections. In addition, relevant experiments of *S. aureus* treated with indirubin-3′-monoxime **5aa**, including TEM analysis, Syto9/PI staining, and the leakage of extracellular potassium ions and nucleic acid (260 nm), have been performed after treatment of *S. aureus* ATCC25923 with indirubin-3′-monoxime **5aa**. The results revealed that indirubin-3′-monoxime **5aa** might show its antibacterial activity by targeting the bacterial membrane and changing the cell membrane permeability of *S. aureus* ATCC25923. The results of cytotoxicity tests of indirubin-3′-monoximes **5aa**, **5r** and **5s** on hepatocytes and SH-SY5Y cells and the skin irritation test of **5aa** on male mice after shaving indicate that indirubin-3′-monoxime **5aa** should be suitable for topical use and could be used as a lead compound of skin antibacterial drugs. This research also represents a typical example of post-modified indirubin derivatives in the field of antibacterial agent research, and further optimization of molecular structure and antibacterial effect, and more thorough and further toxicological studies (such as the mutagenic (genotoxic) potential, carcinogenic, reproductive and developmental toxicity, and neurotoxicity) of indirubin-3′-monoximes are ongoing in our lab.

Experimental section

Chemistry

The chemical solvents and reagents used in synthesis and separation and purification processes were purchased from commercial suppliers (such as Energy-chemical, Alfa, Aladdin). Solvents were of reagent grade, and, when necessary, were purified by standard procedures as specified in Purification of Laboratory Chemicals, 4th edn (Armarego, W. L. F.; Perrin, D. D., Butterworth Heinemann: 1997). All reactions were monitored by analytical thin-layer chromatography (TLC). TLC was performed on silica gel plates with F-254 indicator and compounds were visualized by irradiation with UV light and/or by treatment with a solution of phosphomolybdic acid in ethanol followed by heating. Flash column chromatography was carried out over silica gel (200–300 mesh).

Nuclear magnetic resonance (^{1}H NMR, ^{13}C NMR) spectra were obtained with a JNM-ECS400 (400 M) or 600 MHz Bruker Avance III HD spectrometer (400 or 600 MHz ^{1}H, 101 or 151 MHz ^{13}C). The spectra were recorded in $CDCl_3$ or DMSO-d_6 as the solvents at room temperature. ^{1}H and ^{13}C NMR chemical shifts are reported in ppm relative to the residual solvent peak or TMS as an internal standard: $CDCl_3$ (^{1}H NMR: δ 7.26, singlet; ^{13}C NMR: δ 77.0, triplet), DMSO-d_6 (^{1}H NMR: δ 2.50, singlet, ^{13}C NMR: δ 39.5, multiplet). Data for ^{1}H NMR are reported as follows: chemical shift (δ ppm), multiplicity (s = singlet, d = doublet, t = triplet, m = multiplet, dd = doublet of doublet), integration, coupling constant (Hz) and assignment. Data for ^{13}C NMR are reported as chemical shift.

High-resolution mass spectra (HRMS) were recorded with a WaterXevo G2S QTOF mass spectrometer (ESI) or Thermofisher (Vanquish (UPLC)-Q-Exactive Plus) mass instrument (ESI) and methanol was used to dissolve the samples. HPLC was employed to confirm the purity of compounds to be >95%.

Indirubin-3′-monoximes **5a–z** and **5aa–5ad** were prepared by the following published procedures.[19,22,29,38,55–59]

General procedure for the synthesis of indirubin-3′-monoximes 5a–z and 5aa–5ad

To an aqueous solution of KOH (3.83 g, 68 mmol, 2.3 equiv.) and K_2CO_3 (4.14 g, 30 mmol, 1.0 equiv.) were added the corresponding 2-bromobenzoic acid (6.03 g, 30 mmol, 1.0 equiv.), glycine (3.38 g, 45 mmol, 1.5 equiv.) and copper powder (10.8 mg, 0.15 mmol) under stirring. After the mixture was refluxed for 3–12 h (as judged by TLC analysis), the precipitate was filtered off, and then the filtrate was diluted with 1 N HCl. The precipitate obtained was collected and washed with cold water. The corresponding product **2** was afforded with 48–96% yields through collecting and drying the obtained precipitate.

To a solution of **2** (20 mmol, 1.0 equiv.) and Ac_2O (30 mL, 60 mmol, 3.0 equiv.) was added anhydrous NaOAc (2.46 g, 30 mmol, 1.5 equiv.) under stirring. Then, the above mixture was refluxed for 2–6 h (as judged by TLC analysis) and then cooled to 60 °C to remove Ac_2O under reduced pressure. The corresponding crude product was extracted with ethyl acetate. The collected organic layer was washed with saturated $NaHCO_3$ and brine solution, dried over anhydrous Na_2SO_4 and concentrated *in vacuo* after filtration to give crude product. The crude product was directly purified by flash column chromatography to yield the corresponding 1-acetyl-1*H*-indol-3-yl acetates **3** with 48–80% yields.

Under nitrogen atmosphere, corresponding **3** (3.66 mmol, 1.0 equiv.) and isatin **6** (4.1 mmol, 1.1 equiv.) were dissolved in AcOH (20 mL) and HCl (3.1 mL, 1 mol l^{-1}) under stirring at room temperature. Then, the above reaction mixture was stirred for 12 h at room temperature (as judged by TLC analysis). After the reaction was completed, the mixture was quenched with H_2O. The reddish precipitate was filtered off and recrystallized from 1 N HCl/EtOH solution to afford the corresponding indirubins **4** or **7** with 40–90% yields.

The corresponding indirubin **4** or **7** (5 mmol, 1.0 equiv.) and hydroxylamine hydrochloride (110 mmol, 22.0 equiv.) were

dissolved in pyridine (7 mL), and the reaction mixture was refluxed for several hours until no starting material was detected by TLC. Then, the above mixture was cooled to room temperature and was diluted with 2 N HCl (50 mL) to afford the corresponding reddish solid **5a–z** and **5aa–5ad** with 59–97% yields.

(2*Z*,3*E*)-3-(Hydroxyimino)-[2,3′-biindolinylidene]-2′-one (5a). Red solid; yield: 83%; m.p. 272–273 °C; ^{1}H NMR (400 MHz, DMSO-d_6) δ ppm: 13.49 (s, 1H), 11.74 (s, 1H), 10.72 (s, 1H), 8.65 (d, J = 7.6 Hz, 1H), 8.24 (d, J = 7.6 Hz, 1H), 7.40 (d, J = 4.0 Hz, 2H), 7.13 (td, J = 7.6, 1.2 Hz, 1H), 7.05–6.99 (m, 1H), 6.95 (td, J = 7.6, 1.2 Hz, 1H), 6.90 (d, J = 7.6 Hz, 1H); ^{13}C NMR (100 MHz, DMSO-d_6) δ ppm: 171.0, 151.3, 145.3, 144.9, 138.3, 132.1, 128.0, 125.9, 123.0, 122.7, 121.5, 120.4, 116.5, 111.5, 108.9, 98.9; HRMS (ESI): calcd for $C_{16}H_{11}N_3O_2$ [M + H]$^+$ 278.09240, found 278.09190. HPLC purity 98%.

(2*Z*,3*E*)-3-(Hydroxyimino)-5-methyl-[2,3′-biindolinylidene]-2′-one (5b). Red solid; yield: 90%; m.p. 283–285 °C; ^{1}H NMR (400 MHz, DMSO-d_6) δ ppm: 13.47 (s, 1H), 11.67 (s, 1H), 10.69 (s, 1H), 8.63 (d, J = 8.0 Hz, 1H), 8.07 (s, 1H), 7.27 (d, J = 7.9 Hz, 1H), 7.21 (d, J = 8.2 Hz, 1H), 7.11 (t, J = 7.2 Hz, 1H), 6.94 (t, J = 8.0 Hz, 1H), 6.89 (d, J = 7.6 Hz, 1H), 2.31 (s, 3H); ^{13}C NMR (100 MHz, DMSO-d_6) δ ppm: 171.0, 151.4, 145.7, 142.8, 138.2, 132.6, 130.4, 128.3, 125.7, 122.9, 122.7, 120.4, 116.7, 111.2, 108.8, 98.5, 20.7; HRMS (ESI) m/z calcd for $C_{17}H_{13}N_3O_2$ [M + H]$^+$ 292.10805, found 292.10893. HPLC purity 98%.

(2*Z*,3*E*)-3-(Hydroxyimino)-5-methoxy-[2,3′-biindolinylidene]-2′-one (5c). Red solid; yield: 83%; m.p. >300 °C; ^{1}H NMR (400 MHz, DMSO-d_6) δ ppm: 13.56 (s, 1H), 11.65 (s, 1H), 10.69 (s, 1H), 8.62 (d, J = 7.6 Hz, 1H), 7.82 (d, J = 2.4 Hz, 1H), 7.34 (d, J = 8.8 Hz, 1H), 7.12 (td, J = 7.6, 1.2 Hz, 1H), 7.03 (dd, J = 8.8, 2.8 Hz, 1H), 6.95 (td, J = 8.0, 1.2 Hz, 1H), 6.90 (d, J = 7.6 Hz, 1H), 3.77 (s, 3H); ^{13}C NMR (100 MHz, DMSO-d_6) δ ppm: 170.9, 154.4, 151.5, 145.8, 139.0, 138.1, 125.6, 122.8, 120.3, 118.5, 117.0, 112.8, 112.2, 108.8, 98.2, 55.6; HRMS (ESI) m/z calcd for $C_{17}H_{13}N_3O_3$ [M + H]$^+$ 308.10297, found 308.10303. HPLC purity 97%.

(2*Z*,3*E*)-3-(Hydroxyimino)-5-nitro-[2,3′-biindolinylidene]-2′-one (5d). Red solid; yield: 95%; m.p. >300 °C; ^{1}H NMR (400 MHz, DMSO-d_6) δ ppm: 13.66 (s, 1H), 11.86 (s, 1H), 11.08 (s, 1H), 8.62 (d, J = 8.0 Hz, 1H), 8.23 (d, J = 7.6 Hz, 1H), 7.47–7.38 (m, 2H), 7.16 (dd, J = 8.0, 0.8 Hz, 1H), 7.05 (t, J = 8.0 Hz, 1H), 6.96 (t, J = 8.0 Hz, 1H); ^{13}C NMR (100 MHz, DMSO-d_6) δ ppm: 170.8, 151.3, 146.6, 144.7, 135.3, 132.2, 128.0, 125.2, 124.7, 122.0, 121.4, 121.3, 116.5, 113.3, 111.9, 98.2; HRMS (ESI) m/z calcd for $C_{16}H_{10}N_4O_4$ [M + H]$^+$ 323.07748, found 323.07685. HPLC purity 95%.

(2*Z*,3*E*)-5-Chloro-3-(hydroxyimino)-[2,3′-biindolinylidene]-2′-one (5e). Red solid; yield: 90%; m.p. >300 °C; ^{1}H NMR (400 MHz, DMSO-d_6) δ ppm: 13.80 (s, 1H), 11.73 (s, 1H), 10.75 (s, 1H), 8.61 (d, J = 7.6 Hz, 1H), 8.18 (s, 1H), 7.42 (s, 2H), 7.13 (t, J = 7.6 Hz, 1H), 6.97–6.88 (m, 2H); ^{13}C NMR (100 MHz, DMSO-d_6) δ ppm: 170.9, 150.5, 144.7, 138.7, 131.7, 127.5, 127.2, 126.4, 125.0, 123.2, 122.6, 120.6, 117.8, 113.2, 109.1, 99.8; HRMS (ESI) m/z calcd for $C_{16}H_{10}ClN_3O_2$ [M + H]$^+$ 312.05343, found 312.05244. HPLC purity 97%.

(2*Z*,3*E*)-5-Bromo-3-(hydroxyimino)-[2,3′-biindolinylidene]-2′-one (5f). Red solid; yield: 97%; m.p. 271–274 °C; ^{1}H NMR (400 MHz, DMSO-d_6) δ ppm: 13.74 (s, 1H), 11.75 (s, 1H), 10.75 (s, 1H), 8.62 (d, J = 8.0 Hz, 1H), 8.34 (d, J = 2.0 Hz, 1H), 7.57 (dd, J = 8.4, 2.0 Hz, 1H), 7.40 (d, J = 8.4 Hz, 1H), 7.14 (td, J = 7.6, 0.8 Hz, 1H), 6.95 (td, J = 7.6, 1.2 Hz, 1H), 6.90 (d, J = 7.6 Hz, 1H); ^{13}C NMR (100 MHz, DMSO-d_6) δ ppm: 170.8, 150.3, 149.6, 144.88, 138.6, 136.2, 134.4, 129.9, 126.3, 123.9, 120.5, 118.2, 113.6, 112.5, 108.9, 99.7; HRMS (ESI) m/z calcd for $C_{16}H_{10}BrN_3O_2$ [M + H]$^+$ 356.00292, found 356.00249. HPLC purity 95%.

(2*Z*,3*E*)-6-Fluoro-3-(hydroxyimino)-[2,3′-biindolinylidene]-2′-one (5g). Red solid; yield: 90%; m.p. >300 °C; ^{1}H NMR (400 MHz, DMSO-d_6) δ ppm: 13.75 (s, 1H), 11.81 (s, 1H), 10.87 (s, 1H), 8.59 (d, J = 8.0 Hz, 1H), 8.07 (dd, J = 7.2, 1.2 Hz, 1H), 7.40–7.31 (m, 1H), 7.16 (t, J = 7.6 Hz, 1H), 7.08–7.01 (m, 1H), 6.97 (t, J = 7.6 Hz, 1H), 6.92 (d, J = 7.6 Hz, 1H); ^{13}C NMR (100 MHz, DMSO-d_6) δ ppm: 171.4, 150.5, 146.9 (d, J = 242.0 Hz), 144.8, 138.5, 131.6 (d, J = 13.0 Hz), 126.6, 123.2, 122.4, 122.2, 120.7, 119.7 (d, J = 13.0 Hz), 118.3 (d, J = 16.0 Hz), 109.2, 100.3; HRMS (ESI) m/z calcd for $C_{16}H_{10}FN_3O_2$ [M + H]$^+$ 296.08298, found 296.08249. HPLC purity 95%.

(2*Z*,3*E*)-3-(Hydroxyimino)-6-methoxy-[2,3′-biindolinylidene]-2′-one (5h). Red solid; yield: 87%; m.p. >300 °C; ^{1}H NMR (600 MHz, DMSO-d_6) δ ppm: 13.16 (s, 1H), 11.69 (s, 1H), 10.72 (s, 1H), 8.67 (d, J = 7.8 Hz, 1H), 8.12 (d, J = 8.4 Hz, 1H), 7.12 (t, J = 7.8 Hz, 1H), 7.05 (d, J = 1.8 Hz, 1H), 6.94 (t, J = 7.8 Hz, 1H), 6.90 (d, J = 7.8 Hz, 1H), 6.57 (dd, J = 9.0, 2.4 Hz, 1H), 3.80 (s, 3H); ^{13}C NMR (150 MHz, DMSO-d_6) δ ppm: 171.0, 162.7, 150.8, 146.9, 146.2, 138.3, 129.2, 125.9, 123.2, 122.6, 120.4, 110.3, 108.9, 107.5, 99.0, 97.3, 55.5; HRMS (ESI) m/z calcd for $C_{17}H_{13}N_3O_3$ [M + Na]$^+$ 330.08491, found 330.08415. HPLC purity 96%.

(2*Z*,3*E*)-6-Chloro-3-(hydroxyimino)-[2,3′-biindolinylidene]-2′-one (5i). Red solid; yield: 85%; m.p. >300 °C; ^{1}H NMR (400 MHz, DMSO-d_6) δ ppm: 13.61 (s, 1H), 11.76 (s, 1H), 10.76 (s, 1H), 8.64 (d, J = 7.6 Hz, 1H), 8.20 (d, J = 8.0 Hz, 1H), 7.52 (d, J = 2.0 Hz, 1H), 7.14 (td, J = 7.6, 1.2 Hz, 1H), 7.04 (dd, J = 8.0, 2.0 Hz, 1H), 6.95 (td, J = 7.6, 0.8 Hz, 1H), 6.90 (d, J = 7.6 Hz, 1H); ^{13}C NMR (100 MHz, DMSO-d_6) δ ppm: 170.8, 150.4, 146.2, 144.8, 138.7, 136.2, 129.0, 126.4, 123.3, 122.5, 121.1, 120.5, 115.4, 111.7, 109.0, 100.0; HRMS (ESI) m/z calcd for $C_{16}H_{10}ClN_3O_2$ [M + H]$^+$ 312.05343, found 312.05265. HPLC purity 96%.

(2*Z*,3*E*)-6-Bromo-3-(hydroxyimino)-[2,3′-biindolinylidene]-2′-one (5j). Red solid; yield: 88%; m.p. >300 °C; ^{1}H NMR (600 MHz, DMSO-d_6) δ ppm: 13.63 (s, 1H), 11.75 (s, 1H), 10.77 (s, 1H), 8.64 (d, J = 7.8 Hz, 1H), 8.13 (d, J = 8.4 Hz, 1H), 7.68 (d, J = 1.8 Hz, 1H), 7.18 (dd, J = 8.4, 1.8 Hz, 1H), 7.14 (td, J = 7.2, 1.2 Hz, 1H), 6.95 (td, J = 7.8, 1.2 Hz, 1H), 6.90 (d, J = 7.8 Hz, 1H); ^{13}C NMR (150 MHz, DMSO-d_6) δ ppm: 170.8, 150.5, 146.3, 144.7, 138.7, 129.3, 126.4, 125.0, 124.0, 123.3, 122.5, 120.5, 115.7, 114.5, 109.0, 100.0; HRMS (ESI) m/z calcd for $C_{16}H_{10}BrN_3O_2$ [M + H]$^+$ 356.00291, found 356.00116. HPLC purity 95%.

(2*Z*,3*E*)-3-(Hydroxyimino)-6-nitro-[2,3′-biindolinylidene]-2′-one (5k). Red solid; yield: 70%; m.p. >300 °C; ^{1}H NMR (600 MHz, DMSO-d_6) δ ppm: 14.05 (s, 1H), 11.96 (s, 1H), 10.79 (s, 1H), 8.63 (d, J = 7.8 Hz, 1H), 8.43 (d, J = 8.4 Hz, 1H), 8.31 (d, J = 1.8 Hz, 1H), 7.86 (dd, J = 8.4, 2.4 Hz, 1H), 7.17 (t, J = 7.8 Hz, 1H),

6.96 (t, J = 7.8 Hz, 1H), 6.91 (d, J = 7.8 Hz, 1H); ^{13}C NMR (150 MHz, DMSO-d_6) δ ppm: 170.5, 150.1, 149.4, 145.7, 144.3, 138.9, 128.4, 126.9, 123.3, 122.3, 121.2, 120.6, 116.4, 109.1, 106.7, 100.7; HRMS (ESI) m/z calcd for $C_{16}H_{10}N_4O_4$ $[M + H]^+$ 323.07748, found 323.07589. HPLC purity 95%.

(2*Z*,3*E*)-3-(Hydroxyimino)-6-methyl-[2,3′-biindolinylidene]-2′-one (5l). Red solid; yield: 90%; m.p. 277–280 °C; ^{1}H NMR (400 MHz, DMSO-d_6) δ ppm: 13.37 (s, 1H), 11.65 (s, 1H), 10.70 (s, 1H), 8.64 (d, J = 7.8 Hz, 1H), 8.09 (d, J = 7.8 Hz, 1H), 7.18 (s, 1H), 7.12 (t, J = 7.6 Hz, 1H), 6.92 (dd, J = 7.7, 1.9 Hz, 2H), 6.84 (d, J = 7.8 Hz, 1H), 2.33 (s, 3H); ^{13}C NMR (100 MHz, DMSO-d_6) δ ppm: 171.1, 151.3, 149.6, 145.8, 145.2, 142.5, 138.3, 127.9, 126.0, 123.1, 122.7, 120.5, 114.4, 111.9, 109.0, 98.9, 21.9; HRMS (ESI) m/z calcd for $C_{17}H_{13}N_3O_2$ $[M + H]^+$ 292.10805, found 292.10690. HPLC purity 96%.

(2*Z*,3*E*)-7-Fluoro-3-(hydroxyimino)-[2,3′-biindolinylidene]-2′-one (5m). Red solid; yield: 88%; m.p. >300 °C; ^{1}H NMR (600 MHz, DMSO-d_6) δ ppm: 13.66 (s, 1H), 11.81 (s, 1H), 10.75 (s, 1H), 8.48 (d, J = 11.4 Hz, 1H), 8.23 (d, J = 7.8 Hz, 1H), 7.45–7.38 (m, 2H), 7.08–7.02 (m, 1H), 6.96–6.91 (m, 1H); ^{13}C NMR (100 MHz, DMSO-d_6) δ ppm: 171.1, 157.5 (d, J = 229.5 Hz), 151.4, 146.2, 144.8, 134.6, 132.2, 128.0, 123.8 (d, J = 10.5 Hz), 121.9, 116.5, 111.8, 111.7, 109.7 (d, J = 27.0 Hz), 109.1 (d, J = 9.3 Hz), 98.6; ^{19}F NMR (DMSO-d_6, 376 MHz): δ = −135.93 ppm; HRMS (ESI) m/z calcd for $C_{16}H_{10}FN_3O_2$ $[M + Na]^+$ 318.06493, found 318.06444. HPLC purity 98%.

(2*Z*,3*E*)-3-(Hydroxyimino)-5′-methyl-[2,3′-biindolinylidene]-2′-one (5o). Red solid; yield: 86%; m.p. 288–292 °C; ^{1}H NMR (400 MHz, DMSO-d_6) δ ppm: 13.41 (s, 1H), 11.72 (s, 1H), 10.59 (s, 1H), 8.49 (s, 1H), 8.24 (d, J = 7.6 Hz, 1H), 7.43–7.33 (m, 2H), 7.07–6.98 (m, 1H), 6.94 (dd, J = 7.6, 0.8 Hz, 1H), 2.34 (s, 3H); ^{13}C NMR (100 MHz, DMSO-d_6) δ ppm: 171.1, 151.3, 145.1, 144.9, 136.2, 132.0, 128.9, 128.0, 126.4, 123.7, 122.7, 121.4, 116.5, 111.5, 108.5, 99.2, 21.4; HRMS (ESI) m/z calcd for $C_{17}H_{13}N_3O_2$ $[M + H]^+$ 292.10805, found 292.10668. HPLC purity 97%.

(2*Z*,3*E*)-3-(Hydroxyimino)-5′-methoxy-[2,3′-biindolinylidene]-2′-one (5p). Red solid; yield: 82%; m.p. 263–266 °C; ^{1}H NMR (400 MHz, DMSO-d_6) δ ppm: 13.56 (s, 1H), 11.77 (s, 1H), 10.55 (s, 1H), 8.34 (s, 1H), 8.25 (d, J = 7.6 Hz, 1H), 7.41–7.36 (m, 2H), 7.08–6.98 (m, 1H), 6.79 (d, J = 8.4 Hz, 1H), 6.72 (dd, J = 8.4, 2.8 Hz, 1H), 3.77 (s, 3H); ^{13}C NMR (100 MHz, DMSO-d_6) δ ppm: 171.1, 154.2, 151.5, 145.3, 144.8, 132.3, 132.1, 128.1, 123.5, 121.5, 116.6, 111.5, 111.3, 109.6, 1008.9, 99.5, 55.6; HRMS (ESI) m/z calcd for $C_{17}H_{13}N_3O_3$ $[M + H]^+$ 308.10297, found 308.10258. HPLC purity 95%.

(2*Z*,3*E*)-3-(Hydroxyimino)-5′-nitro-[2,3′-biindolinylidene]-2′-one (5q). Red solid; yield: 83%; m.p. 258–262 °C; ^{1}H NMR (400 MHz, DMSO-d_6) δ ppm: 13.89 (s, 1H), 11.87 (s, 1H), 11.41 (s, 1H), 9.45 (s, 1H), 8.25 (d, J = 7.6 Hz, 1H), 8.07 (d, J = 8.8 Hz, 1H), 7.49–7.40 (m, 2H), 7.12–7.02 (m, 2H); ^{13}C NMR (100 MHz, DMSO-d_6) δ ppm: 171.1, 151.7, 147.4, 144.5, 143.4, 141.6, 132.2, 128.1, 123.0, 122.4, 122.0, 117.7, 116.5, 112.2, 108.6, 96.7; HRMS (ESI) m/z calcd for $C_{16}H_{10}N_4O_4$ $[M + H]^+$ 323.07748, found 323.07661. HPLC purity 99%.

(2*Z*,3*E*)-5′-Fluoro-3-(hydroxyimino)-[2,3′-biindolinylidene]-2′-one (5r). Red solid; yield: 85%; m.p. 295–297 °C; ^{1}H NMR (600 MHz, DMSO-d_6) δ ppm: 13.68 (s, 1H), 11.82 (s, 1H), 10.85 (s, 1H), 8.65 (s, 1H), 8.24 (d, J = 7.2 Hz, 1H), 7.45–7.38 (m, 2H), 7.17–7.12 (m, 1H), 7.08–7.02 (m, 1H), 6.89 (d, J = 8.4 Hz, 1H); ^{13}C NMR (150 MHz, DMSO-d_6) δ ppm: 170.7, 151.4, 146.4, 144.7, 136.8, 132.2, 128.0, 125.1, 124.7, 124.3, 122.1, 121.9, 116.5, 111.8, 109.9, 97.8; HRMS (ESI) m/z calcd for $C_{16}H_{10}FN_3O_2$ $[M + H]^+$ 296.08298, found 296.08176. HPLC purity 97%.

(2*Z*,3*E*)-5′-Chloro-3-(hydroxyimino)-[2,3′-biindolinylidene]-2′-one (5s). Red solid; yield: 83%; m.p. 296–299 °C; ^{1}H NMR (400 MHz, DMSO-d_6) δ ppm: 13.70 (s, 1H), 11.84 (s, 1H), 10.87 (s, 1H), 8.77 (d, J = 1.7 Hz, 1H), 8.24 (d, J = 7.6 Hz, 1H), 7.42 (t, J = 9.1 Hz, 2H), 7.27 (dd, J = 8.2, 1.9 Hz, 1H), 7.05 (t, J = 7.3 Hz, 1H), 6.85 (d, J = 8.2 Hz, 1H); ^{13}C NMR (100 MHz, DMSO-d_6) δ ppm: 170.8, 151.5, 146.4, 144.7, 136.9, 132.2, 128.0, 125.2, 124.7, 124.3, 122.2, 122.0, 116.5, 111.9, 110.0, 97.8; HRMS (ESI) m/z calcd for $C_{16}H_{10}ClN_3O_2$ $[M + H]^+$ 312.05343, found 312.05257. HPLC purity 96%.

(2*Z*,3*E*)-5′-Bromo-3-(hydroxyimino)-[2,3′-biindolinylidene]-2′-one (5t). Red solid; yield: 80%; m.p. >300 °C; ^{1}H NMR (600 MHz, DMSO-d_6) δ ppm: 13.70 (s, 1H), 11.84 (s, 1H), 10.87 (s, 1H), 8.77 (s, 1H), 8.24 (d, J = 7.8 Hz, 1H), 7.45–7.38 (m, 2H), 7.27 (dd, J = 8.4, 1.8 Hz, 1H), 7.05 (t, J = 7.2 Hz, 1H), 6.85 (d, J = 8.4 Hz, 1H); ^{13}C NMR (150 MHz, DMSO-d_6) δ ppm: 170.6, 151.5, 146.4, 144.7, 137.2, 132.2, 128.0 (128.04, 127.97), 124.8, 122.0, 116.5, 112.7, 111.9, 110.5, 97.7; HRMS (ESI) m/z calcd for $C_{16}H_{10}BrN_3O_2$ $[M + H]^+$ 356.00292, found 356.00261. HPLC purity 99%.

(2*Z*,3*E*)-3-(Hydroxyimino)-5′-iodo-[2,3′-biindolinylidene]-2′-one (5u). Red solid; yield: 59%; m.p. >300 °C; ^{1}H NMR (400 MHz, DMSO-d_6) δ ppm: 13.69 (s, 1H), 11.81 (s, 1H), 10.83 (s, 1H), 8.89 (d, J = 1.6 Hz, 1H), 8.23 (d, J = 7.6 Hz, 1H), 7.47–7.36 (m, 3H), 7.09–7.01 (m, 1H), 6.75 (d, J = 8.0 Hz, 1H); ^{13}C NMR (100 MHz, DMSO-d_6) δ ppm: 170.5, 151.6, 146.4, 144.7, 137.7, 134.0, 132.3, 130.4, 128.1, 125.3, 122.0, 116.6, 111.9, 111.2, 97.5, 84.0; HRMS (ESI) m/z calcd for $C_{16}H_{10}IN_3O_2$ $[M + H]^+$ 403.98905, found 403.98760. HPLC purity 95%.

(2*Z*,3*E*)-3-(Hydroxyimino)-6′-methoxy-[2,3′-biindolinylidene]-2′-one (5v). Red solid; yield: 85%; m.p. 256–257 °C; ^{1}H NMR (400 MHz, DMSO-d_6) δ ppm: 13.29 (s, 1H), 11.46 (s, 1H), 10.68 (s, 1H), 8.57 (d, J = 8.4 Hz, 1H), 8.22 (d, J = 7.6 Hz, 1H), 7.41–7.34 (m, 2H), 7.03–6.94 (m, 1H), 6.53–6.47 (m, 2H), 3.77 (s, 3H); ^{13}C NMR (100 MHz, DMSO-d_6) δ ppm: 171.5, 158.5, 151.3, 145.1, 143.0, 140.1, 131.9, 128.0, 124.3, 121.0, 116.5, 115.8, 111.3, 106.0, 99.3, 95.3, 55.2; HRMS (ESI) m/z calcd for $C_{17}H_{13}N_3O_3$ $[M + H]^+$ 308.10297, found 308.10258. HPLC purity 99%.

(2*Z*,3*E*)-3-(Hydroxyimino)-7′-methyl-[2,3′-biindolinylidene]-2′-one (5w). Red solid; yield: 78%; m.p. 258–262 °C; ^{1}H NMR (400 MHz, DMSO-d_6) δ ppm: 13.45 (s, 1H), 11.79 (s, 1H), 10.73 (s, 1H), 8.52 (d, J = 8.0 Hz, 1H), 8.24 (d, J = 7.6 Hz, 1H), 7.40 (d, J = 4.0 Hz, 1H), 7.06–6.99 (m, 1H), 6.95 (d, J = 7.6 Hz, 1H), 6.87 (t, J = 7.6 Hz, 1H), 2.27 (s, 1H); ^{13}C NMR (100 MHz, DMSO-d_6) δ ppm: 171.4, 151.4, 145.2, 144.8, 136.9, 132.0, 128.0, 127.3, 122.3, 121.4, 120.6, 120.3, 117.9, 116.5, 111.5, 99.5, 16.5; HRMS (ESI) m/z calcd for $C_{17}H_{13}N_3O_2$ $[M + H]^+$ 292.10805, found 292.10663. HPLC purity 99%.

(2*Z*,3*E*)-7′-Fluoro-3-(hydroxyimino)-[2,3′-biindolinylidene]-2′-one (5x). Red solid; yield: 90%; m.p. >300 °C; ^{1}H NMR (600 MHz, DMSO-d_6) δ ppm: 13.63 (s, 1H), 11.84 (s, 1H), 11.17 (s, 1H), 8.50

(d, J = 7.8 Hz, 1H), 8.23 (d, J = 7.2 Hz, 1H), 7.48–7.38 (m, 2H), 7.08–6.98 (m, 2H), 6.96–6.91 (m, 1H); ^{13}C NMR (100 MHz, DMSO-d_6) δ ppm: 170.8, 151.3, 146.7, 144.7, 135.3, 132.2, 128.0, 125.2, 124.7, 122.0, 121.4, 121.3, 116.5, 113.3, 111.9, 98.0; ^{19}F NMR (DMSO-d_6, 376 MHz): δ = −134.68 ppm; HRMS (ESI) m/z calcd for $C_{16}H_{10}FN_3O_2$ $[M + H]^+$ 296.08298, found 296.08188. HPLC purity 99%.

(2*Z*,3*E*)-7′-Chloro-3-(hydroxyimino)-[2,3′-biindolinylidene]-2′-one (5y). Red solid; yield: 82%; m.p. >300 °C; ^{1}H NMR (600 MHz, DMSO-d_6) δ ppm: 13.66 (s, 1H), 11.86 (s, 1H), 11.08 (s, 1H), 8.63 (d, J = 7.8 Hz, 1H), 8.23 (d, J = 7.8 Hz, 1H), 7.47–7.39 (m, 2H), 7.17 (d, J = 8.4 Hz, 1H), 7.06 (t, J = 7.2 Hz, 1H), 6.96 (t, J = 7.8 Hz, 1H); ^{13}C NMR (100 MHz, DMSO-d_6) δ ppm: 170.8, 151.3, 146.6, 144.7, 135.3, 132.2, 128.0, 125.2, 124.7, 122.0, 121.4, 121.3, 116.5, 113.3, 111.9, 98.2; HRMS (ESI) m/z calcd for $C_{16}H_{10}ClN_3O_2$ $[M + H]^+$ 312.05343, found 312.05347. HPLC purity 99%.

(2*Z*,3*E*)-7′-Bromo-3-(hydroxyimino)-[2,3′-biindolinylidene]-2′-one (5z). Red solid; yield: 85%; m.p. 291–294 °C; ^{1}H NMR (600 MHz, DMSO-d_6) δ ppm: 13.65 (s, 1H), 11.87 (s, 1H), 10.93 (s, 1H), 8.67 (d, J = 7.8 Hz, 1H), 8.23 (d, J = 7.8 Hz, 1H), 7.47–7.39 (m, 2H), 7.29 (d, J = 8.0 Hz, 1H), 7.06 (t, J = 7.2 Hz, 1H), 6.91 (t, J = 7.8 Hz, 1H); ^{13}C NMR (150 MHz, DMSO-d_6) δ ppm: 170.6, 151.3, 146.6, 144.6, 136.9, 132.1, 128.1, 127.9, 124.6, 122.0, 121.8, 121.6, 116.4, 111.9, 101.5, 98.3; HRMS (ESI) m/z calcd for $C_{16}H_{10}BrN_3O_2$ $[M + H]^+$ 356.00292, found 356.00231. HPLC purity 99%.

(2*Z*,3*E*)-3-(Hydroxyimino)-7′-(trifluoromethyl)-[2,3′-biindolinylidene]-2′-one (5aa). Red solid; yield: 85%; m.p. >300 °C; ^{1}H NMR (600 MHz, DMSO-d_6) δ ppm: 13.76 (s, 1H), 11.92 (s, 1H), 11.13 (s, 1H), 8.94 (d, J = 7.8 Hz, 1H), 8.24 (d, J = 7.2 Hz, 1H), 7.49–7.35 (m, 3H), 7.14–7.04 (m, 2H); ^{13}C NMR (150 MHz, DMSO-d_6) δ ppm: 171.2, 151.4, 147.0, 144.6, 134.6, 132.2, 127.9, 126.0, 124.6, 124.1 (q, J = 270.0 Hz), 122.2, 121.5, 120.2, 116.5, 112.0, 109.9 (q, J = 33.0 Hz), 96.6; ^{19}F NMR (DMSO-d_6, 376 MHz): δ = −59.80 ppm; HRMS (ESI) m/z calcd for $C_{17}H_{10}F_3N_3O_2$ $[M + H]^+$ 346.07979, found 346.07883. HPLC purity 99%.

(2*Z*,3*E*)-3-(Hydroxyimino)-5-methoxy-7′-(trifluoromethyl)-[2,3′-biindolinylidene]-2′-one (5ab). Red solid; yield: 85%; m.p. >300 °C; ^{1}H NMR (600 MHz, DMSO-d_6) δ ppm: 13.81 (s, 1H), 11.86 (s, 1H), 11.09 (s, 1H), 8.90 (d, J = 7.8 Hz, 1H), 8.58 (d, J = 5.4 Hz, 1H), 7.82 (d, J = 8.4 Hz, 1H), 7.41 (d, J = 9.0 Hz, 1H), 7.10 (t, J = 7.8 Hz, 1H), 7.06 (dd, J = 8.4, 2.4 Hz, 1H), 3.78 (s, 3H); ^{13}C NMR (150 MHz, DMSO-d_6) δ ppm: 171.0, 154.9, 151.5, 149.6, 147.4, 138.6, 136.1, 134.71, 125.6, 124.7, 124.1 (q, J = 270.0 Hz), 123.9, 120.0, 117.0, 112.7 (d, J = 9.0 Hz), 109.8 (q, J = 31.5 Hz), 95.9, 55.6; HRMS (ESI) m/z calcd for $C_{18}H_{12}F_3N_3O_3$ $[M + H]^+$ 374.075799, found 374.07675. HPLC purity 98%.

(2*Z*,3*E*)-5-Chloro-3-(hydroxyimino)-7′-(trifluoromethyl)-[2,3′-biindolinylidene]-2′-one (5ac). Red solid; yield: 75%; m.p. >300 °C; ^{1}H NMR (600 MHz, DMSO-d_6) δ ppm: 13.99 (s, 1H), 11.93 (s, 1H), 11.15 (s, 1H), 8.89 (d, J = 7.8 Hz, 1H), 8.19 (d, J = 1.8 Hz, 1H), 7.78 (t, J = 7.8 Hz, 1H), 7.52–7.46 (m, 2H), 7.39 (d, J = 7.8 Hz, 1H), 7.11 (t, J = 7.8 Hz, 1H); ^{13}C NMR (150 MHz, DMSO-d_6): δ 171.0, 150.5, 149.6, 146.3, 143.5, 136.1, 131.7, 127.0, 126.0, 125.6, 124.4, 124.1 (q, J = 270.0 Hz), 120.2, 117.6, 113.5, 109.9 (q, J = 31.5 Hz), 97.4; HRMS (ESI) m/z calcd for $C_{17}H_9ClF_3N_3O_2$ $[M + H]^+$ 378.026262, found 378.02704. HPLC purity 97%.

(2*Z*,3*E*)-5-Bromo-3-(hydroxyimino)-7′-(trifluoromethyl)-[2,3′-biindolinylidene]-2′-one (5ad). Red solid; yield: 88%; m.p. >300 °C; ^{1}H NMR (600 MHz, DMSO-d_6): δ 14.00 (s, 1H), 11.93 (s, 1H), 11.15 (s, 1H), 8.89 (d, J = 7.8 Hz, 1H), 8.58 (s, 1H), 8.33 (d, J = 2.4 Hz, 1H), 7.61 (dd, J = 7.8, 2.4 Hz, 1H), 7.46 (d, J = 8.4 Hz, 1H), 7.11 (t, J = 7.8 Hz, 1H); ^{13}C NMR (150 MHz, DMSO-d_6): δ 171.0, 150.4, 149.4, 146.1, 143.8, 136.4, 134.5, 129.8, 126.0, 124.4, 124.1 (q, J = 270.0 Hz), 124.0, 120.2, 118.1, 114.1, 113.3, 109.9 (q, J = 31.5 Hz), 97.4; HRMS (ESI) m/z calcd for $C_{17}H_9BrF_3N_3O_2$ $[M + H]^+$ 421.975748, found 421.97703. HPLC purity 96%.

Antibacterial susceptibility assays

The MICs of the test compounds were determined using the broth microdilution procedure described in the Clinical and Laboratory Standards Institute (CLSI) guidelines.[62] Strains of *E. coli* ATCC 25922, *S. aureus* ATCC 25923, *P. aeruginosa* ATCC9027, and clinically isolated multi-drug-resistant strain of *S. aureus* (20 151 027 077) were incubated in MHB for 16–24 h at 37 °C and were diluted to 1 × 10^6 CFU mL^{-1}. The starting concentration of indirubin-3′-oxime derivatives was set as 204.8 μg mL^{-1}, then two-fold dilution of samples was made in 96-well plates (the ending concentration was 0.2 μg mL^{-1}, 100 μL in each well), then 100 μL test microorganism was added to the wells and was incubated for 16 h at 37 °C. A final concentration of 0.25% Resaxurin (7-sodiooxy-3*H*-phenoxazin-3-one 10-oxide) in wells as microorganism growth indictor was added and continuously incubated for 3 h before MIC reading. Equivalent amounts of DMSO (5%) and medium were successively used as negative controls and blank control. Levofloxacin was used as a positive drug. All experiments were performed in three replicates.

MBC assay

MBC assay was conducted using the broth microdilution assay described in the preceding section.[69,70] After the 24 h incubation period, aliquots from microtiter wells were plated onto MHA. The colonies that grew after 24 h of incubation were counted, with MBC being defined as the lowest compound concentration resulting in a ≥3-log reduction in the number of colony forming units (CFU).

Drug combination of indirubin-3′-oxime derivatives and levofloxacin on multi-drug-resistant strain of *S. aureus*

The combination effects between indirubin-3′-oxime derivatives and antibiotic (levofloxacin) were determined with a checkerboard assay.[63,71] Two-fold serial dilutions of indirubin-3′-oxime derivatives (50 μL) were prepared in vertical rows of a 96-well plate, and two-fold serial dilutions of the antibiotic (50 μL) were added in the horizontal orientation rows of the 96-well plate. The concentrations of each compound and antibiotic ranged from 2 to 1/32 of their MICs. Subsequently, 100 μL of 1 × 10^6 CFU mL^{-1} bacterial inoculum was added in each well. Then, 100 μL of each MHB and 1 × 10^6 CFU mL^{-1} bacterial inoculum

were added in wells as reference. The combinatory effects were then determined based on the FICI values calculated according to the formula: FICI = FIC(A) + FIC(B), where FIC is defined as the MIC of samples/drugs in combination divided by the MIC of the samples/drugs used alone. The results were considered to be synergistic when FICI $\leq$ 0.5, additive when 0.5 $\leq$ FICI $\leq$ 1, indifferent when 1 $\leq$ FICI $\leq$ 4, and antagonistic when FICI > 4.

TEM analysis of *S. aureus* treated with 5aa

TEM assays were performed to elucidate the impact of indirubin-3′-oxime derivative **5aa** on *S. aureus* microbial cells.[64] After the antibacterial assay, *S. aureus* treated with 12.8 μg mL^{-1} **5aa** was centrifuged at 5000×*g* and 27 °C for 10 min, while the suspension untreated with **5aa** was used as a control. The cells were washed with phosphate buffer (0.1 M PBS, pH = 7.4) for 3 times and then resuspended. Then, the samples were fixed in 2.5% buffered glutaraldehyde solution at 4 °C for 4 h. Finally, the samples were cut with an ultramicrotome (Ultracut UCT, Leica, Wetzlar, Germany). Each sample was evaluated by TEM (HT7800, HITACHI, Japan).

Fluorescence microscope observations of *S. aureus* in the presence and absence of 5aa

50 mL cultures of *S. aureus* bacteria were grown to late log phase in MHB broth with or without **5aa**. Then, 30 mL of the bacterial culture was concentrated by centrifugation at 10 000×*g* for 5–10 minutes. The supernatant was removed and the pellet resuspended in 3 mL of 0.85% NaCl. Then, 1.5 mL of this suspension was added to each of two 30–40 mL centrifuge tubes containing 30 mL of 0.85% NaCl. Both samples were incubated at room temperature for 1 hour, mixing every 15 minutes. Pellets of both samples were obtained by centrifugation at 10 000×*g* for 10–15 minutes. The pellets were resuspended in 30 mL of 0.85% NaCl and centrifuged again at 10 000×*g* for 10–15 minutes. Two pellets were resuspended in separate tubes with 10 mL of 0.85% NaCl each. The optical density was determined at 670 nm (OD_{670}) of a 3 mL aliquot of the bacterial suspensions in glass or acrylic absorption cuvettes (1 cm pathlength). A sample of the 2× stock Syto9/PI staining solution was combined with an equal volume of the bacterial suspension. The final concentration of each dye was 6 μM SYTO 9 stain and 30 μM propidium iodide. Samples were mixed thoroughly and incubated at room temperature in the dark for 15 minutes. Then, 5 μL of the stained bacterial suspension was trapped between a slide and an 18 mm square coverslip. Observation was made with a fluorescence microscope and the excitation/emission maxima for these dyes are about 480/500 nm for SYTO 9 stain and 490/635 nm for propidium iodide. The background remains virtually nonfluorescent.[74]

Assay of extracellular potassium ions

The amount of potassium ion (K^+) outflow was determined according to the method reported in the literature.[65] *S. aureus* cell suspensions were prepared as previously described. Then, different amounts of compound **5aa** were added to the suspension so that the final compound concentrations were 0, 2 MIC, 4 MIC and 8 MIC, respectively. The bacterial suspension was centrifuged. The extracellular potassium concentrations were measured in the supernatant by using a microplate reader and a potassium assay kit following the manufacturer's protocols.

Determination of nucleic acid concentration

Leakages of nucleic acid from *S. aureus* cells were monitored by measuring ultraviolet absorbance at 260 nm using a Shimadzu UV-1800 spectrometer.[66] In brief, after incubating for 8 h treated with 0, 2 MIC, 4 MIC and 8 MIC of **5aa**, the samples were centrifuged and the supernatant was taken. The supernatant was filtered through a microporous membrane and measured for OD_{260} nm using a UV spectrophotometer. The difference between four recordings of data at 260 nm is the final result of nucleic acid leakage from *S. aureus*.

Determination of antibacterial zone diameter

The antibacterial zone diameter test was performed according to the CLSI method.[62]

Cell safety evaluation in SH-SY5Y cells

Using indirubin and levofloxacin as positive drugs, CCK-8 assay was used to test the *in vitro* inhibitory activity of the target molecule against SH-SY5Y cells. The SH-SY5Y cells were seeded in 96-well plates and incubated for 24 h. Medium containing test drugs was added according to groups, and solvent group and positive control group were set up. After 72 h of treatment, 10 μL CCK-8 solution was added to each well and incubated for 3 h. The absorbance value (OD) of each well was measured at 450 nm with a microplate reader, and the cell survival rate was calculated.[75]

Skin irritation test

Skin tolerance tests were done using the Organization for Economic Cooperation and Development guidelines with slight modification. Twenty-four hours before the experiment, fur from the backs of all mice was clipped at different sites (Fig. 7). 12.8 μg mL^{-1} **5aa** was evenly and gently applied in a test site while untreated skin areas served as the control. The test sites were then examined critically at 1 h after removing the test material and at 24 h, 48 h and 72 h for dermal reaction using Draize scoring criteria.[76] All experiments were performed according to the national and institutional guidelines and approved by the Animal Care Welfare Committee of Guizhou Medical University (no. 2100168). The experimental mice were Kunming mice purchased from Guizhou Laboratory Animal Engineering Technology Center (purchase order no. 20002).

Conflicts of interest

All the authors declare that they have no conflict of interest.

Acknowledgements

We thank the following for the financial support of this work: National Natural Science Foundation of China (no. 22061011, U1812403-05 and 81960628), Guizhou Science and Technology Department of China (no. QKHJC[2020]1Y031 and QKHRCPT [2017]5101), Guizhou Health Committee (gzwjkj2020-1-209), the State Key Laboratory of Functions and Applications of Medicinal Plants (no. FAMP201904K), and the Cultivation Project of National Natural Science Foundation of Guizhou Medical University (no. 20NSP054).

Notes and references

1 G. Dhanda, P. Sarkar, S. Samaddar and J. Haldar, *J. Med. Chem.*, 2019, **62**, 3184.
2 J. N. Pendleton, S. P. Gorman and B. F. Gilmore, *Expert Rev. Anti-Infect. Ther.*, 2013, **11**, 297.
3 E. Montassier, R. Valdés-Mas, E. Batard, N. Zmora, M. Dori-Bachash, J. Suez and E. Elinav, *Nat. Microbiol.*, 2021, **6**, 1043.
4 Interagency Coordination Group on Antimicrobial Resistance, *Report to the Secretary-General of the United Nations*, 2019.
5 E. Montassier, R. Valdés-Mas, E. Batard, N. Zmora, M. Dori-Bachash, J. Suez and E. Elinav, *Nat. Microbiol.*, 2021, **6**, 1043.
6 B. Kongkham, D. Prabakaran and H. Puttaswamy, *Fitoterapia*, 2020, **147**, 104762.
7 B. Casciaro, L. Mangiardi, F. Cappiello, I. Romeo, M. R. Loffredo, A. Iazzetti, A. Calcaterra, A. Goggiamani, F. Ghirga, M. L. Mangoni, B. Botta and D. Quaglio, *Molecules*, 2020, **25**, 3619.
8 S. N. Khadake, S. Karamathulla, T. K. Jena, M. Monisha, N. K. Tuti, F. A. Khan and R. Anindya, *Bioorg. Med. Chem. Lett.*, 2021, **39**, 127883.
9 D. Hughes and A. Karlen, *Upsala J. Med. Sci.*, 2014, **119**, 162.
10 J. O'Neill, *Review on Antimicrobial Resistance*, 2016.
11 F. J. Álvarez-Martínez, E. Barrajón-Catalán and V. Micol, *Biomedicines*, 2020, **8**, 405.
12 R. Tommasi, D. G. Brown, G. K. Walkup, J. I. Manchester and A. A. Miller, *Nat. Rev. Drug Discovery*, 2015, **14**, 529.
13 T. Efferth, P. C. H. Li, V. S. B. Konkimalla and B. Kaina, *Trends Mol. Med.*, 2007, **13**, 353.
14 Y.-Y. Tu, *Angew. Chem., Int. Ed.*, 2016, **55**, 10210.
15 D. J. Newman, *Adv. Pharmacol.*, 2020, **87**, 113.
16 F. J. Álvarez-Martínez, E. Barrajón-Catalán and V. Micol, *Biomedicines*, 2020, **8**, 405.
17 Q.-Y. Yang, T. Zhang, Y.-N. He, S.-J. Huang, X. Deng, L. Han and C.-G. Xie, *Chin Med.*, 2020, **15**(1), 127.
18 D. J. Newman and G. M. Cragg, *J. Nat. Prod.*, 2012, **75**, 311.
19 R. Hoessel, S. Leclerc, J. A. Endicott, M. E. Nobel, A. Lawrie, P. Tunnah, M. Leost, E. Damiens, D. Marie, D. Marko, E. Niederberger, W. Tang, G. Eisenbrand and L. Meijer, *Nat. Cell Biol.*, 1999, **1**, 60.
20 N. Stasiak, W. Kukula-koch and K. Glowniak, *Acta Pol. Pharm.*, 2014, **71**, 215.
21 X. Cheng and K. H. Merz, *Adv. Exp. Med. Biol.*, 2016, **929**, 269.
22 H.-Z. Wang, Z.-Y. Wang, C.-Y. Wei, J. Wang J, Y.-S. Xu, G.-H. Bai, Q.-Z. Yao, L. Zhang and Y.-Z. Chen, *Eur. J. Med. Chem.*, 2021, **223**, 113652.
23 B. Sun, J.-H. Wang, L.-H. Liu, L.-F. Mao, L.-Z. Peng and Y.-W. Wang, *Chem. Biol. Drug Des.*, 2021, **97**, 565.
24 W. L. Hsieh, Y.-K. Lin, C. N. Tsai, T.-M. Wang, T. Y. Chen and J. H. S. Pang, *J. Dermatol. Sci.*, 2012, **67**, 140.
25 J.-L. Lai, Y.-H. Liu, C. Liu, M.-P. Qi, R.-N. Liu, X.-F. Zhu, Q.-G. Zhou, Y.-Y. Chen, A.-Z. Guo and C.-M. Hu, *Inflammation*, 2017, **40**, 1.
26 T.-J. Qi, H.-T. Li and S. Li, *Oncotarget*, 2017, **8**, 6658.
27 M. H. Kim, Y. Y. Choi, G. Yang, I. H. Cho, D. Nam and W. M. Yang, *J. Ethnopharmacol.*, 2013, **145**, 214.
28 X. Cheng, K. H. Merz, S. Vatter, J. Zeller, S. Muehlbeyer, A. Thommet, J. Christ, S. Wölfl and G. Eisenbrand, *J. Med. Chem.*, 2017, **60**, 4949.
29 Z.-X. Cao, F.-F. Yang, J. Wang, Z.-C. Gu, S.-X. Lin, P. Wang, J.-X. An, T. Liu, Y. Li, Y.-J. Li, H.-N. Lin, Y.-L. Zhao and B. He, *J. Med. Chem.*, 2021, **60**, 15280.
30 H. Pandraud, *Bull. Soc. Chim. Fr.*, 1961, **7**, 1257.
31 S. J. Choi, J. E. Lee, S. Y. Jeong, I. Im, S. D. Lee, E. J. Lee, S. K. Lee, S. M. Kwon, S. G. Ahn, J. H. Yoon, S. Y. Han, J. I. Kim and Y. C. Kim, *J. Med. Chem.*, 2010, **53**, 3696.
32 K. Vougogiannopoulou, Y. Ferandin, K. Bettayeb, V. Myrianthopoulos, O. Lozach, Y. Fan, C. H. Johnson, P. Magiatis P, A. L. Skaltsounis, E. Mikros and L. Meijer, *J. Med. Chem.*, 2008, **51**, 6421.
33 Y. Ferandin, K. Bettayeb, M. Kritsanida, O. Lozach, P. Polychronopoulos, P. Magiatis, A. L. Skaltsounis and L. Meijer, *J. Med. Chem.*, 2006, **49**, 4638.
34 F. P. Guengerich, J. L. Sorrells, S. Schmitt, J. A. Krauser, P. Aryal and L. Meijer, *J. Med. Chem.*, 2004, **47**, 3236.
35 P. Polychronopoulos, P. Magiatis, A. L. Skaltsounis, V. Myrianthopoulos, E. Mikros, A. Tarricone, A. Musacchio, S. M. Roe, L. Pearl, M. Leost, P. Greengard and L. Meijer, *J. Med. Chem.*, 2004, **47**, 935.
36 C. L. Woodard, Z. Li, A. K. Kathcart, J. Terrell, L. Gerena, M. Lopez-Sanchez, D. E. Kyle, A. K. Bhattacharjee, D. A. Nichols, W. Ellis, S. T. Prigge, J. A. Geyer and N. C. Waters, *J. Med. Chem.*, 2003, **46**, 3877.
37 E. Gerometta, I. Grondin, J. Smadja, M. Frederich and A. Gauvin-Bialecki, *J. Ethnopharmacol.*, 2020, **253**, 112608.
38 X. Cheng, P. Rasqué, S. Vatter, K. H. Merz and G. Eisenbrand, *Bioorg. Med. Chem.*, 2010, **18**, 4509.
39 L. Meijer, A. L. Skaltsounis, P. Magiatis, P. Polychronopoulos, M. Knockaert, M. Leost, X. P. Ryan, C. A. Vonica, A. Brivanlou, R. Dajani, C. Crovace, C. Tarricone, A. Musacchio, S. M. Roe, L. Pearl and P. Greengard, *Chem. Biol.*, 2003, **10**, 1255.
40 Y. K. Chan, H. H. Kwok, L. S. Chan, K. S. Leung, J. Shi, N. K. Mak, R. N. Wong and P. Y. Yue, *Biochem. Pharmacol.*, 2012, **83**, 598.
41 S. Nam, R. Buettner, J. Turkson, D. Kim, J. Q. Cheng, S. Muehlbeyer, F. Hippe, S. Vatter, K. H. Merz, G. Eisenbrand and R. Jove, *Proc. Natl. Acad. Sci. U. S. A.*, 2005, **102**, 5998.

42 S. Nam, A. Scuto, F. Yang, W. Chen, S. Park, H. S. Yoo, H. Konig, R. Bhatia, X. Cheng, K. H. Merz, G. Eisenbrand and R. Jove, *Mol. Oncol.*, 2012, **6**, 276.

43 S. Nam, W. Wen, A. Schroeder, A. Herrmann, H. Yu, X. Cheng, K. H. Merz, G. Eisenbrand, H. Li, Y. C. Yuan and R. Jove, *Mol. Oncol.*, 2013, **7**, 369.

44 A. Walter, A. Chaikuad, R. Helmer, N. Loaec, L. Preu, I. Ott, S. Knapp, L. Meijer and C. Kunick, *PLoS One*, 2018, **13**(5), e0196761.

45 W. L. Hsieh, Y.-K. Lin, C. N. Tsai, T.-M. Wang, T. Y. Chen and J. H. S. Pang, *J. Dermatol. Sci.*, 2012, **67**, 140.

46 T. Kunikata, T. Tatefuji, H. Aga, K. Iwaki, M. Ikeda and M. Kurimoto, *Eur. J. Pharmacol.*, 2000, **410**, 93.

47 R. Jautelat, T. Brumby, M. Schafer, H. Briem, G. Eisenbrand, S. Schwahn, M. Kruger, U. Lucking, O. Prien and G. Siemeister, *ChemBioChem*, 2005, **6**, 531.

48 P. Kannan, B. Shanmugavadivu, C. Petchiammal and W. Hopper, *Acta Bot. Hung.*, 2006, **48**, 323.

49 P. Kannan, R. Mohankumar, S. Ignacimuthu and M. G. Paulraj, *Scand. J. Infect. Dis.*, 2010, **42**, 500.

50 K. Ponnusamy, C. Petchiammal, R. Mohankumar and W. Hopper, *J. Ethnopharmacol.*, 2010, **132**, 349.

51 Y. R. Chiang, A. Li, Y. L. Leu, J. Y. Fang and Y. K. Lin, *Molecules*, 2013, **18**, 14381.

52 S. K. Mahendra and P. V. Nityanand, *J. Coastal Life Med.*, 2014, **2**(10), 826.

53 K. V. Devika, T. Sabarinathan and S. Shamala, *J. Orofacial Sci.*, 2021, **13**, 67.

54 B. Sun, J.-H. Wang, L.-H. Liu, L.-F. Mao, L.-Z. Peng and Y.-W. Wang, *Chem. Biol. Drug Des.*, 2021, **97**, 565.

55 C. Pergola, N. Gaboriaud-Kolar, N. Jestadt, S. Konig, M. Kritsanida, A. M. Schaible, H. Li, U. Garscha, C. Weinigel, D. Barz, K. F. Albring and O. Huber, *J. Med. Chem.*, 2014, **57**, 3715.

56 V. Myrianthopoulos, P. Magiatis, Y. Ferandin, A. L. Skaltsounis, L. Meijer and E. Mikros, *J. Med. Chem.*, 2007, **50**, 4027.

57 T. Blažević, E. H. Heiss, A. G. Atanasov, J. M. Breuss, V. M. Dirsch and P. Uhrin, *Evid. Based Complementary Altern. Med.*, 2015, **2015**, 654098.

58 T. R. Kameswaran and R. Ramanibai, *Biomed. Pharmacother.*, 2009, **63**, 146.

59 X.-M. Liao and K.-N. Leung, *Oncol Rep.*, 2013, **29**(1), 371–379.

60 B. S. Jenie, B. P. Priosoeryanto, R. Syarief and G. T. Rekso, *Hayati*, 2008, **15**, 56.

61 V. K. Bajpai, K. H. Baek and S. C. Kang, *Food Res. Int.*, 2012, **45**, 722.

62 M. A. Wikler, *Approved Standard*, 2009, M7-A8.

63 S. Mulyaningsih, F. Sporer, S. Zimmermann, J. Reichling and M. Wink, *Phytomedicine*, 2010, **17**, 1061.

64 W.-C. Zeng WC, Q. He, Q. Sun, K. Zhong and H. Gao, *Int. J. Food Microbiol.*, 2012, **153**, 78.

65 A. Sharma, V. K. Bajpai and K. Baek, *J. Food Saf.*, 2013, **33**, 197.

66 H.-Y. Cui, C.-H. Zhang, C.-Z. Li and L. Lin, *Ind. Crops Prod.*, 2019, **139**, 111498.

67 Clinical and Laboratory Standards Institute, *CLSI*, 2018, M07Ed11.

68 M. M. F. Ismail, H. G. Abdulwahab, E. S. Nossier, N. G. E. Menofy and B. A. Abdelkhalek, *Bioorg. Chem.*, 2020, **94**, 103437.

69 F.-C. Bi, D. Song, N. Zhang, Z.-Y. Liu, X.-J. Gu, C.-Y. Hu, X.-K. Cai, H. Venter and S.-T. Ma, *Eur. J. Med. Chem.*, 2018, **159**, 90.

70 D. Song, F.-C. Bi, N. Zhang, Y.-H. Qin, X.-B. Liu, Y.-T. Teng and S.-T. Ma, *Bioorg. Med. Chem.*, 2020, **28**(21), 115729.

71 Z. Li, J. Tu, G.-Y. Han, N. Liu and C.-Q. Sheng, *J. Med. Chem.*, 2021, **64**(2), 1116.

72 G.-H. Li, Y.-F. Xu, X. Wang, B.-G. Zhang, C. Shi, W.-S. Zhang and X.-D. Xia, *Foodborne Pathog. Dis.*, 2014, **11**, 314.

73 A. Sharma, V. K. Bajpai and K. Baek, *J. Food Saf.*, 2013, **33**, 197.

74 D. Meier, M. V. Hernández, L. Geelen, R. Muharini, P. Proksch and J. E. Bandow, *Bioorg. Med. Chem.*, 2019, **27**, 115151.

75 J. Zhang, Z. Zhang, W. Song and J. Liu, *Mol. Cell. Probes*, 2020, **52**, 101566.

76 V. A. Nyigo, R. Mdegela, F. Mabiki and H. M. Malebo, *Eur. J. Med. Plants*, 2015, **10**, 1.

77 A. Mekonnen, S. Tesfaye, S. G. Christos, K. Dires, T. Zenebe, N. Zegeye, Y. Shiferaw and E. Lulekal, *J. Toxicol.*, 2019, **2019**, 1.